SF2A 2021
A. Siebert, K. Baillié, E. Lagadec, N. Lagarde, J. Malzac, J.-B. Marquette, M. N'Diaye, J. Richard, O. Venot (eds)

CONSTRAINING THE DUST GRAIN ALIGNMENT MECHANISM(S) RESPONSIBLE FOR THE (SUB-)MILLIMETER DUST POLARIZATION OBSERVED IN CLASS 0 PROTOSTELLAR CORES

V. J. M. Le Gouellec[1,2], A. J. Maury[2,3] and C. L. H. Hull[4,5,6]

Abstract. With the aim of characterizing the role played by magnetic fields in the formation of young protostars, several recent studies have revealed unprecedented features toward high angular resolution ALMA dust polarization observations of Class 0 protostellar cores. Especially, the dust polarization has been found to be enhanced along the irradiated cavity walls of bipolar outflows, but also in region most likely linked with the infalling envelope, in the form of filamentary structure being potential magnetized accretion streamer. These observations allow us to investigate the physical processes involved in the Radiative Alignment Torques (RATs) acting on dust grains from the core to disk scales. Synthetic observations of non-ideal magneto-hydrodynamic simulations of protostellar cores implementing RATs, show that the ALMA values of grain alignment efficiency lie among those predicted by a perfect alignment of grains, and are significantly higher than the ones obtained with the standard RAT alignment of paramagnetic grains. Ultimately, our results suggest dust alignment mechanism(s) are efficient at producing polarized dust emission in the local conditions typical of Class 0 protostars. However, further study leading to a better characterization of dust grain characteristics, or additional grain alignment mechanisms, will be required to investigate the cause of strong polarized dust emission located in regions of the envelope where alignment conditions are not favorable. A new attempt aiming at a better characterization of the dust grain alignment mechanism(s) occurring in young star forming objects, is to investigate the chemistry going on in those cores, and see if the local physical conditions (irradiation, temperature) can reconcile both molecular line emission and dust polarization observations.

Keywords: ISM: jets and outflows – ISM: magnetic fields – polarization – stars: formation – stars: magnetic field – stars: protostars

1 Introduction

Protostellar formation is ruled by various competing dynamical processes. Once a prestellar core has undergone gravitational collapse, a protostar is formed; the so-called Class 0 phase corresponds to the stage when the protostar is accreting material from the surrounding envelope. During this phase, the magnetic field is thought to regulate the collapse of the envelope redistributing the angular momentum. A variety of mechanisms have been proposed to explain the removal of angular momentum from the rotating envelope, including binary formation via turbulent fragmentation (Offner et al. 2010), as well as the launching of jets and outflows. These processes are intimately linked with the magnetic field, which has the capability to extract angular momentum from the rotating core via magnetic braking, which in turn can suppress the formation of large disks at early times (Hennebelle & Ciardi 2009). In addition, magnetic field morphology in the inner core of protostars have been found to be affected by protostellar outflows, suggesting magnetic fields can be dynamically overwhelmed by the outflowing activity (Hull et al. 2017).

[1] European Southern Observatory, Alonso de Córdova 3107, Vitacura, Santiago, Chile
[2] AIM, CEA, CNRS, Université Paris-Saclay, Université Paris Diderot, Sorbonne Paris Cité, F-91191 Gif-sur-Yvette, France
[3] Harvard-Smithsonian Center for Astrophysics, Cambridge, MA 02138, USA
[4] National Astronomical Observatory of Japan, NAOJ Chile Observatory , Alonso de Córdova 3788, Office 61B, 7630422, Vitacura, Santiago, Chile
[5] Joint ALMA Observatory, Alonso de Córdova 3107, Vitacura, Santiago, Chile
[6] NAOJ Fellow

At the spatial scales now probed by ALMA, one can access to the magnetic field morphology of the inner regions of Class 0 protostellar cores. One way to characterize the morphology of magnetic fields is to observe the polarized thermal emission from dust grains. Indeed, since dust grains are not perfectly spherical, they tend to align themselves with the ambient magnetic field under some conditions via the action of Radiative Alignment Torques (RATs, (Lazarian & Hoang 2007; Andersson et al. 2015)). This linear polarization emanating from this dust grain population is orthogonal to the magnetic field component projected on the plane of the sky, and integrated along the line of sight. The aim of our work is to assess whether RATs are efficient at producing the polarized dust emission revealed by ALMA observations toward the interior of star forming cores, and if additional grain alignment mechanisms can occur. This requires a deep understanding of the physical conditions of these regions.

2 ALMA dust polarization observations

The recent ALMA observations of Class 0 envelopes revealed a variety of magnetic field morphology, toward specific regions of the core where the polarized dust emission was found to be strongly enhanced, namely the walls of the bipolar outflow cavities, filament-like structures that are potential magnetized accretion streamers, and core equatorial planes (Hull et al. 2017; Maury et al. 2018; Sadavoy et al. 2018a,b; Kwon et al. 2019; Takahashi et al. 2019; Le Gouellec et al. 2019; Hull et al. 2020). An example is shown if Figure 1, where we present ALMA observations of two Class 0 star forming cores located in the Serpens Main star forming region, Serpens Emb 8(N) and Serpens SMM1 (Le Gouellec et al. 2019). Serpens Emb 8(N), a low-mass protostellar core, exhibits enhanced polarized dust emission surrounding the two outflow lobes, suggesting an organized magnetic field. The core appears axisymmetric, and a powerful extremely high velocity (EHV) jet is launched from the central protostellar regions. Serpens SMM1 corresponds to a clump of cores, whose central one SMM1-a, is an intermediate-mass protostellar core, and launches a broad low-velocity outflow as well as an EHV jet of the redshifted side. The polarized dust emission is very different, with notably two crossing highly polarized filament-like structures to the South of the source. One is thought to correspond to an outflow cavity walls, while the other is more likely a streaming funnelling material to the central hot-corino.

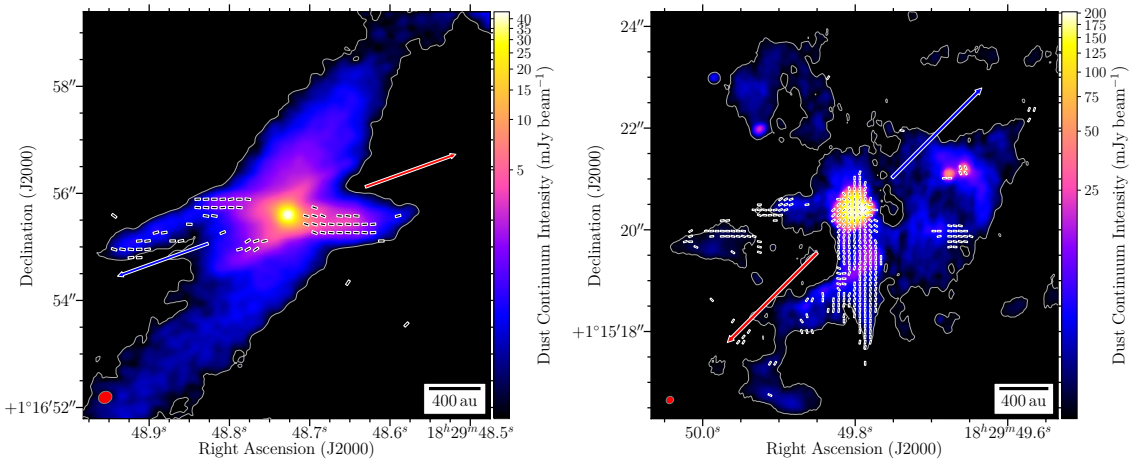

Fig. 1. Magnetic field around Serpens Emb 8(N) (left panel) and Serpens SMM1 (right panel) from (Le Gouellec et al. 2019). Line segments represent the magnetic field orientation. The color scale is the total intensity (Stokes I) of the thermal dust emission. The blue and red arrows represent the directions of the blueshifted and redshifted lobes of the bipolar outflow, respectively. The polarized emission is clearly enhanced along the outflow cavity walls visible here in the dust thermal emission.

3 Estimating the dust grain alignment efficiency

These highly polarized structures raised several questions concerning the grain alignment mechanism responsible for this grain alignment. The average level of fractional polarization $\mathcal{P}_{\rm frac}$ was high compared to what was expected from RATs, and the thermal emission is only polarized toward specific regions of the inner core. A

solution has been to consider both the effects of interferometric filtering, and the impact of the disorganized component of the apparent magnetic along the line-of-sight, on the measurement of polarization fraction. To do so we applied the method developed in Planck Collaboration et al. (2020) for *Planck* observations, on a set of ALMA observations of Class 0 cores (Le Gouellec et al. 2020). The disorganized component of the apparent magnetic impacts the dispersion of polarization position angle in the plane of the sky $\mathcal{S}$, and the depolarization along the line-of-sight. The idea is that assuming this disorganized component is isotropic, one could correct its impact on the depolarization measured in the polarization fraction, multiplying $\mathcal{P}_{\rm frac}$ by $\mathcal{S}$.

As shown in Figure 2, we compare the values of $\mathcal{S} \times \mathcal{P}_{\rm frac}$ in the ALMA observations, with MHD models of protostars performed with collaborators with the state of-the-art RAMSES code, synthetically observed by the polarization radiative transfer code POLARIS (Reissl et al. 2016). Our analysis resulted in the discovery that the grain alignment efficiency is approximately constant across the three orders of magnitude in envelope column density probed by the ALMA observations. Thanks to these comparisons, we also found that the ALMA values of grain alignment efficiency are notably higher than what the classical RAT theory can produce, and are typically reaching values reproduced if we assume perfect alignment (PA) in our models. We concluded that a more detailed understanding of the dust grain characteristics and/or the proof that additional grain alignment mechanisms are occurring, will be required to complete our picture of dust polarization.

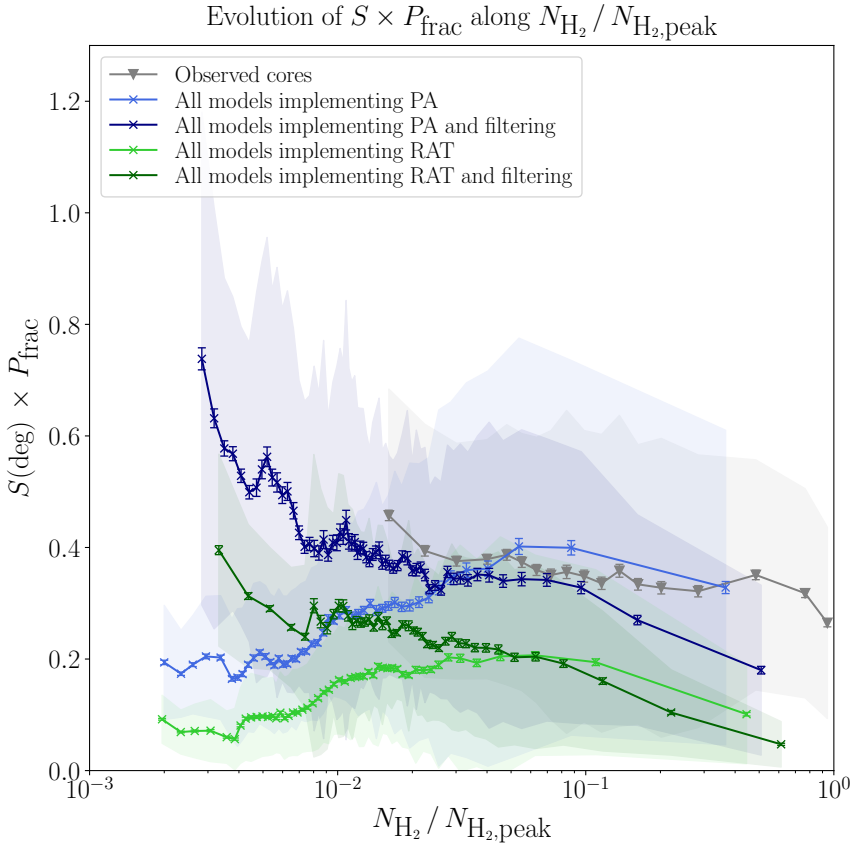

Fig. 2. Observed distributions of the mean values of $\mathcal{S} \times \mathcal{P}_{\rm frac}$ as a function of the column density $N_{\rm H_2}$ (normalized by its maximum value, $N_{\rm H_2,peak}$) of ALMA observations of Class 0 protostellar cores (triangles) and of MHD models (crosses) synthetically observed by the radiative transfer code POLARIS. The four lines representing the simulations correspond to results using RATs or perfect alignment (PA), both filtered and not filtered. The shaded areas represent the standard deviation of the Gaussian fit performed on each bin of points. The error bars correspond to these standard deviation values divided by the square root of the number of points in each bin. Taken from Le Gouellec et al. (2020).

4 Radiative transfer modelling of polarized dust emission

To reproduce the high level of grain alignment efficiency measured in ALMA observations, we developed further detailed MHD models to first reproduce the structures of the inner regions in Class 0 envelope, i.e. outflow cavity walls and filament-like accreting structures. Thanks to POLARIS, we can vary several parameters, linked to the dust grain characteristics (their size, shape and paramagnetic susceptibility) as well as to the local conditions of irradiation. The aim in to target the conditions that would reproduce the behavior of grains aligned by RATs. If RATs is responsible for the polarization we observe, we need to implement large grains (≥ 10 μm in size), super-paramagnetic grains (to ensure that a large fraction of grains rotate suprathermally), and high irradiation conditions (central luminosity ≥ 20 $L_\odot$) in our models of intermediate-mass protostellar cores to increase the grain alignment efficiency, which is still not entirely reproduced. This encourages us to investigate further mechanisms, such as mechanically aligned grains (Hoang et al. 2018), grain aligned with the radiation field anisotropy (Lazarian & Hoang 2007), and rotational disruption of grains (Hoang et al. 2019), in order to reconcile dust polarization observations and our knowledge of dust characteristics, grain alignment mechanisms, and local conditions, on the interior of protostars. An ultimate goal will be to compare these constrains on the environmental conditions in the interior of protostars with the results brought by the analysis of molecular emission lines detected toward these regions. Several molecules (like hydrocarbons chains such as C_2H or c-C_3H_2), whose chemical formation pathway requires significant irradiation have been detected toward outflow cavities. Qualitative comparisons between the polarized dust emission and the emission from such molecules could bring further clues on the characteristics of the aligned dust grains dust and magnetic fields of the inner regions of Class 0 protostellar cores.

References

Andersson, B.-G., Lazarian, A., & Vaillancourt, J. E. 2015, ARA&A, 53, 501
Hennebelle, P. & Ciardi, A. 2009, A&A, 506, L29
Hoang, T., Cho, J., & Lazarian, A. 2018, ApJ, 852, 129
Hoang, T., Tram, L. N., Lee, H., & Ahn, S.-H. 2019, Nature Astronomy, 3, 766
Hull, C. L. H., Girart, J. M., Tychoniec, Ł., et al. 2017, ApJ, 847, 92
Hull, C. L. H., Le Gouellec, V. J. M., Girart, J. M., Tobin, J. J., & Bourke, T. L. 2020, ApJ, 892, 152
Kwon, W., Stephens, I. W., Tobin, J. J., et al. 2019, ApJ, 879, 25
Lazarian, A. & Hoang, T. 2007, MNRAS, 378, 910
Le Gouellec, V. J. M., Hull, C. L. H., Maury, A. J., et al. 2019, ApJ, 885, 106
Le Gouellec, V. J. M., Maury, A. J., Guillet, V., et al. 2020, A&A, 644, A11
Maury, A. J., Girart, J. M., Zhang, Q., et al. 2018, MNRAS, 477, 2760
Offner, S. S. R., Kratter, K. M., Matzner, C. D., Krumholz, M. R., & Klein, R. I. 2010, ApJ, 725, 1485
Planck Collaboration, Aghanim, N., Akrami, Y., et al. 2020, A&A, 641, A12
Reissl, S., Wolf, S., & Brauer, R. 2016, A&A, 593, A87
Sadavoy, S. I., Myers, P. C., Stephens, I. W., et al. 2018a, ApJ, 859, 165
Sadavoy, S. I., Myers, P. C., Stephens, I. W., et al. 2018b, ApJ, 869, 115
Takahashi, S., Machida, M. N., Tomisaka, K., et al. 2019, ApJ, 872, 70